

Cubic nonlinear susceptibilities of crystals in the optical band; the signs and magnitudes of the susceptibilities of crystals with and without centers of inversion

S. A. Akhmanov, L. B. Meisner, S. T. Parinov, S. M. Saltiel, and V. G. Tunkin

Moscow State University

(Submitted 13 May 1977)

Zh. Eksp. Teor. Fiz. 73, 1710-1728 (November 1977)

A technique has been developed for measuring the modulus and sign of the cubic nonlinear susceptibility, $\chi^{(3)}$, in crystals with and without a center of inversion. The anisotropy coefficient of the $\chi^{(3)}$ tensor in a KDP crystal and the moduli and signs of the elements of the $\chi^{(3)}$ tensor of the CaCO_3 crystal have been measured for the first time. The obtained data are compared with the results of a calculation carried out with the aid of a phenomenological model of the cubic nonlinear susceptibility and the so-called Coulomb-anharmonicity model. The large discrepancies in the values of the various elements of the $\chi^{(3)}$ tensor in a calcite crystal are explained. The data, obtained in the present work, on the cubic susceptibility of a calcite crystal are used to interpret the results of the measurements of the fifth order—in the field—nonlinearities in this crystal.

PACS numbers: 75.30.Cr

§1. INTRODUCTION

The study of cubic susceptibilities is the central problem of nonlinear spectroscopy. Such methods of nonlinear spectroscopy as the two-photon spectroscopy, saturation spectroscopy, and Raman-active scattering spectroscopy are based on effects due to the cubic susceptibility. Therefore, of particular interest at present is information about the cubic-susceptibility tensor $\chi^{(3)}$ for gases,^[1] liquids,^[2] and crystals. In the case of crystals, such data are also of considerable interest for the presently rapidly developing theory of nonlinear optical properties of solids. The great successes achieved by this theory in the explanation of effects quadratic in the field, which are described by the tensor $\chi^{(2)}$, make the performance of similar investigations of the higher-order nonlinearities advisable. Special interest is aroused here by the fact that, using the methods of nonlinear optics, we can obtain information about the electron shells of crystals that is not accessible to other methods (e.g., about the anisotropy in cubic crystals; see below). It should be said, however, that even for the susceptibility $\chi^{(3)}$ only the first steps have been taken in this direction; and what is more, many of the problems connected with the methods of measuring nonlinear susceptibilities (the modulus and sign) have not been completely solved, especially for crystals without a center of inversion. In the last case the main difficulty encountered in the measurement of the components of the $\chi^{(3)}$ tensor is the interference between the direct processes (on the $\chi^{(3)}$ nonlinearity) and the cascade processes due to the interactions on the quadratic nonlinearity.^[3] The possibility of separating the direct and the cascade processes is quite limited^[3,4]; more often than not their interference is very substantial. Therefore, the neglect of the contribution of the cascade processes has led in a number of investigations to incorrect estimates for the cubic susceptibilities.^[6,14]

In fact, there are available in the literature only isolated data for such an important parameter as the sign

of the cubic nonlinear susceptibilities of crystals^[5,8]; in these experiments only the relative sign of $\chi^{(3)}$ was measured. In the present work we have developed the correct technique for measuring the modulus and sign of the $\chi^{(3)}$ susceptibility in crystals with and without a center of inversion. Using it, we have for the first time measured the anisotropy coefficient of the $\chi^{(3)}$ tensor of a KDP crystal and the moduli and signs of the $\chi^{(3)}$ components for a CaCO_3 crystal. The obtained data are compared with theoretical models. Special attention is given to the phenomenological model proposed in Ref. 9 and the Coulomb-anharmonicity model.^[10] It is shown that this model is capable of explaining the large discrepancies in the values of the various components. The data on the $\chi^{(3)}$ of calcite are used to interpret the results obtained earlier by us^[11] in the measurement of the $\chi^{(5)}$ tensor of calcite.

§2. THIRD-HARMONIC GENERATION IN CRYSTALS WITHOUT AN INVERSION CENTER; THE EFFECTIVE NONLINEAR SUSCEPTIBILITY AND THE CONDITIONS FOR SYNCHRONISM

In the present section we present the results of the theoretical investigation of third-harmonic generation in crystals without a center of inversion. The chief characteristics we wish to pay attention to are: the large number of cascade processes, which turn out to be synchronous, and the quite complicated expressions for the effective nonlinear susceptibilities.

The system of equations for the complex amplitudes, A_i , describing third-harmonic generation in media without an inversion center has the following form^[12]:

$$\begin{aligned} \partial A_1 / \partial z &= 0, & \partial A_2 / \partial z &= -i\sigma A_1^2(z) \exp(i\Delta_2 z), \\ \partial A_3 / \partial z &= -i\sigma_c A_1(z) A_2(z) \exp(i\Delta_c z) - i\beta A_1^3(z) \exp(i\Delta_3 z). \end{aligned} \quad (1)$$

The indices 1, 2, 3 refer respectively to the pump, the second harmonic, and the third harmonic; σ and σ_c are the second-order coupling coefficients for second-har-

monic generation and the cascade generation of the third harmonic; β is the third-order coupling coefficient. The phase detunings are expressible in terms of the wave numbers:

$$\Delta_2 = k_2 - 2k_1, \quad \Delta_3 = k_3 - k_2 - k_1, \quad \Delta_3 = k_3 - 3k_1.$$

The solution to the system (1) indicates the existence of three types of synchronous interactions. Each of them is characterized by an appropriate synchronism angle and an effective third-order nonlinearity.

Interaction I

- a) Condition for synchronism: $\Delta_2 = 0$;
 b) field of the third harmonic

$$E_3(z) = \frac{4\pi^2}{n_3\lambda_3} \chi_{\text{eff}}^{(3)} A_1^2 \exp \left[i \left(\omega t - 3k_1 z + \frac{\pi}{2} \right) \right]; \quad (2)$$

- c) effective cubic nonlinearity

$$\chi^{(3)} = \frac{4\pi^2 \langle \chi^{(2)} \rangle_z \langle \chi^{(2)} \rangle_c}{n_3\lambda_3 \Delta_c}, \quad (2a)$$

where $\langle \chi^{(2)} \rangle_z$ and $\langle \chi^{(2)} \rangle_c$ are the contractions of the $\chi^{(2)}$ tensor with respect to the vectors of the waves interacting in the $\omega + \omega = 2\omega$ and $\omega + 2\omega = 3\omega$ processes respectively.

Interaction II

- a) $\Delta_c = 0$;
 b) $E_3(z) = \frac{4\pi^2}{n_3\lambda_3} \chi_{\text{eff}}^{(3)} A_1^2 \exp \left[i \left(\omega t - k_3 z - \frac{\pi}{2} \right) \right]; \quad (3)$
 c) $\chi_{\text{eff}}^{(3)} = \frac{4\pi^2 \langle \chi^{(2)} \rangle_z \langle \chi^{(2)} \rangle_c}{n_3\lambda_3 \Delta_2}. \quad (3a)$

Interaction III

- a) $\Delta_3 = 0$;
 b) $E_3(z) = \frac{4\pi^2}{n_3\lambda_3} \chi_{\text{eff}}^{(3)} A_1^2 \exp \left[i \left(\omega t - 3k_1 z - \frac{\pi}{2} \right) \right]; \quad (4)$
 c) $\chi_{\text{eff}}^{(3)} = \langle \chi^{(3)} \rangle + \frac{4\pi^2 \langle \chi^{(2)} \rangle_z \langle \chi^{(2)} \rangle_c}{n_3\lambda_3 \Delta_c}. \quad (4a)$

Here $\langle \chi^{(3)} \rangle$ is the contraction of $\chi^{(3)}$ with respect to the vectors of the waves participating in the synchronous $\omega + \omega + \omega = 3\omega$ process.

In the directions defined by the condition $\Delta_3 = 0$, the generation of the third harmonic occurs both on account of a straightforward frequency multiplication on the $\chi^{(3)}$ nonlinearity and on account of frequency combination on the $\chi^{(2)}$ nonlinearity. In spite of the fact that the two stages of the cascade process are nonsynchronous, as a whole the process is synchronous, since the equality $\Delta_2 + \Delta_c = \Delta_3 = 0$ is fulfilled.

§3. PROCEDURE FOR MEASURING THE MAGNITUDES AND SIGNS OF THE $\chi^{(3)}$ TENSOR COMPONENTS

3.1. Measurement of the modulus of $\chi^{(3)}$

The existence in crystals without an inversion center of several types of synchronous interactions can be ef-

fectively used to measure the modulus of $\chi^{(3)}$. The principle underlying the measurements^[11,13] consists in the following. Since there exist in a crystal directions in which the effective cubic nonlinearity contains only $\chi^{(2)}$, i. e., in which $\chi_{\text{eff}}^{(3)} \sim |\chi^{(2)}|^2$, and other directions in which $\chi_{\text{eff}}^{(3)} \sim \chi^{(3)} + \alpha |\chi^{(2)}|^2$, the measurement of the ratio of the intensities of the third-harmonic signals in two such directions can be used to determine the magnitude of $\chi^{(3)}$.

The cubic susceptibility is determined from the following equality:

$$\chi_i^{(3)} + \frac{4\pi^2 \langle \chi_i^{(2)} \rangle_z \langle \chi_i^{(2)} \rangle_c}{n_2\lambda_2 \Delta_c} = \pm \frac{4\pi^2 \langle \chi_r^{(2)} \rangle_z \langle \chi_r^{(2)} \rangle_c}{n_2\lambda_2 \Delta_j} \left[\frac{I_3(\Delta_3=0)}{I_3(\Delta_j=0)} \right]^{1/2}, \quad (5)$$

where Δ_j stands for Δ_c or Δ_2 , depending on the form of the cascade process that is used in the measurement, $\chi_i^{(2)}$ and $\chi_r^{(2)}$ are the nonlinear susceptibilities of the crystal under investigation, and $\chi_r^{(2)}$ is the nonlinear susceptibility of the reference crystal.

In measuring $\chi^{(3)}$ in a crystal without an inversion center, we can use as the standard the experimental crystal itself. The expression (5) in this case leads to two possible values for $\chi^{(3)}$. This indeterminacy can be eliminated by measuring the sign of the effective third-order susceptibility.

In measuring $\chi^{(3)}$ in crystals with a center of inversion, as the reference crystal, we can use any noncentrosymmetric crystal with known $\chi^{(2)}$. Since $\chi_i^{(2)} = 0$, only the indeterminacy in the sign of $\chi^{(3)}$ remains.

Let us now consider the method that was used in the measurement of the signs of the components of the third-order nonlinear-susceptibility tensors.

3.2. Measurement of the signs of the $\chi^{(3)}$ components

To measure the signs of the $\chi^{(3)}$ components, we used a method based on the interference of the fields of the third harmonic generated in two crystals positioned one after the other.^[5] Unlike Wynne,^[5] we worked in the synchronous regime, using as the reference crystal a KDP crystal set up in the direction of synchronism defined by the condition $\Delta_2 = 0$ or $\Delta_c = 0$. In these two cases $\chi_{\text{eff}}^{(3)} \sim d_{14}^2$ (KDP), and this allows the direct determination of the sign of $\chi^{(3)}$ in the crystal under investigation. The reference crystal can be any crystal without an inversion center, for which $\langle \chi^{(2)} \rangle_z$ and $\langle \chi^{(2)} \rangle_c$ contain one and the same $\chi^{(2)}$ -tensor component or one and the same combination of the components of the tensor. If this condition is not fulfilled, then it is necessary to know the signs of the $\chi^{(2)}$ components in the reference crystal.

The arrangement of the elements when there is interference between the fields is shown in Fig. 1. The order of the crystals depends on which type of cascade process is used as the reference signal. In the case when the reference crystal is set up in the direction defined by the condition $\Delta_2 = 0$, it should be in front of the crystal being investigated; if, on the other hand, the process

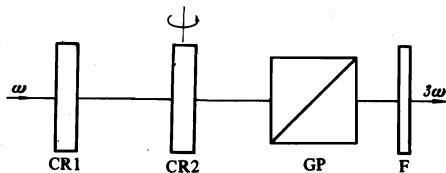


FIG. 1. Experimental scheme for the measurement of the signs of nonlinear susceptibilities: CR1 and CR2 are the reference and experimental crystals; GP, a Glan prism; F, a filter.

with the synchronism condition $\Delta_c = 0$ is used, then the reference crystal should be behind the experimental crystal. Only in the case of such experimental geometry will the interference of the fields not depend on the crystal thicknesses. Let the crystal located in the second place rotate about the direction of exact synchronism. Then, adding up the fields (2), or (3), and (4) of the third harmonic generated in the two crystals, and going over to the intensities, we obtain for the total intensity the expression

$$I_3 = I_3^{(1)} \left[1 + \left(m \frac{\sin \psi}{\psi} \right)^2 + 2m\rho \cos(\psi + \Delta\alpha) \right], \quad (6)$$

where $I_3^{(1)}$ is the third-harmonic intensity in the first crystal only, $m = A_3^{(2)}/A_3^{(1)}$ is the ratio of the third-harmonic amplitudes in the second and first crystals, $\psi = \Delta_3^{(2)} L^{(2)}/2$ is the detuning from exact synchronism in the second crystal, $\Delta\alpha = (k_3^{(a)} - 3k_1^{(a)})L^{(a)}$ is the phase gain in the air space between the crystals.

The coefficient ρ depends on the scheme of the experiment, and assumes the value $\rho = -1$ when the reference process with the synchronism condition $\Delta_2 = 0$ is used and $\rho = +1$ for the reference process with the condition $\Delta_c = 0$.

The synchronism curve for the second crystal differs from the normal dependence $(\sin\psi/\psi)^2$. As can be seen from (6), the shape of the synchronism curve is determined by the distance between the crystals, the sign of the product $m\rho$, and the magnitude of m .

As the reference crystal, we can also use a crystal with an inversion center for which the sign of $\chi^{(3)}$ is

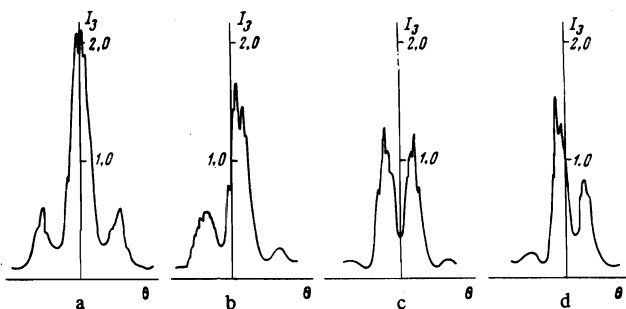


FIG. 2. Synchronism curves for third-harmonic generation in the case when there is interference with an external third-harmonic signal. The curves correspond to different distances between the crystals (see Fig. 1): a) 31 mm, $\Delta\alpha = 2\pi$; b) 39 mm, $\Delta\alpha = 5\pi/2$; c) 46 mm, $\Delta\alpha = 3\pi$; d) 54 mm, $\Delta\alpha = 7\pi/2$.

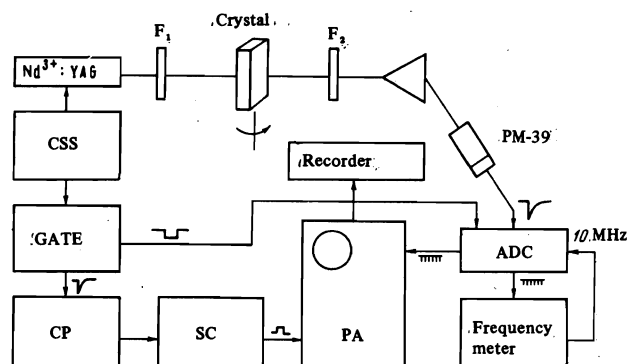


FIG. 3. Block diagram of the experimental setup for the measurement of the magnitudes and signs of nonlinear susceptibilities: F_1 and F_2 —filters, CSS—control system for the laser shutter, GATE—gating pulse shaper, ADC—analogue-digital converter, CP—counter with a pre-unit (F5007); PA—multi-channel pulse analyzer (NTA-1024), SC—shaper of the pulses that switch the PA channels.

known. Then the order in which the crystals set up along the direction defined by the condition $\Delta_3 = 0$ are arranged is immaterial. The coefficient ρ in this case is equal to +1.

In Fig. 2 we show experimental synchronism curves for two identical processes differing in intensity by a factor of five ($m = 2.21$). The curves were measured for different distances between the crystals. The obtained experimental plots correspond to the derived expression (6). In practice the crystals are set up at a distance apart to which corresponds $\Delta\alpha = 2\pi N$. We then determine the sign of m from the shape of the obtained curve (Fig. 2, a or c) and thereby determine whether the signs of $\chi_{eff}^{(3)}$ for the two crystals are the same or different.

§4. DESCRIPTION OF THE EXPERIMENTAL SETUP

A block diagram of the experimental setup is shown in Fig. 3. As the pump we use radiation from a Nd^{3+} -doped garnet laser ($\lambda = 1.064 \mu$) operating on the zero transverse mode in the Q-switched regime. The diameter of the pumping beam at the exit mirror of the laser is ~ 1 mm. The crystal under investigation were located in the near laser-radiation zone. During the measurement of the sign of the components of the nonlinear-susceptibility tensor the pump passes through the two crystals, which stand one after the other at a distance of roughly 10 cm apart. The crystal spacing can be varied. The crystals are rotated with the aid of fractional-horsepower motors with reduction gears for the measurement of the synchronism curves.

The radiation of the third or fourth harmonic is separated out with the aid of a LiF prism, and is recorded on a 39a photomultiplier. The signal from the photomultiplier anode proceeds to an emitter follower and then to an analog-code converter. The analog-code converter is gated by a pulse from a gating-pulse shaper. The duration of the gating pulse is $0.6 \mu\text{sec}$. The gating-pulse shaper is triggered by a pulse from the laser control system.

TABLE I. Possible synchronous third-harmonic generation processes in a KDP crystal.

Interaction number	Synchronism condition	First cascade	Second cascade	Optimal azimuthal angle φ	Synchronism angle θ
1	$k_3^e = 3k_1^o$	$o_{10}o_1 - e_3$	$o_{10}o_1 - e_3$	$\pi/8$	65°
2	\gg	$o_{10}o_1 - e_2$	$e_2o_1 - e_3$	$\pi/8$	
3	$k_2^e = 2k_1^o$	$o_{10}o_1 - e_2$	$e_2o_1 - e_3$	$\pi/8$	41°11'
4	\gg	\gg	$e_2e_1 - o_3$	$\pi/8$	
5	\gg	\gg	$e_2o_1 - o_3$	$\pi/4$	
6	\gg	\gg	$e_2e_1 - e_3$	$\pi/4$	
7	$k_2^e = k_1^e + k_1^o$	$o_1e_1 - e_2$	$e_2o_1 - e_3$	0	58°06'
8	\gg	\gg	$e_2e_1 - o_3$	0	
9	\gg	\gg	$e_2o_1 - o_3$	$\pi/8$	
10	\gg	\gg	$e_1e_1 - e_3$	$\pi/8$	
11	$k_3^e = k_1^e + k_2^o$	$e_1e_1 - o_2$	$e_1o_2 - e_3$	0	58°18'
12	\gg	$o_1e_1 - o_2$	\gg	$\pi/8$	
13	$k_3^e = k_1^o + k_2^o$	$e_1e_1 - o_2$	$o_1o_2 - e_3$	$\pi/8$	47°
14	\gg	$o_1e_1 - o_2$	\gg	0	

The code pulses from the analog-code converter are fed to the input section of a ChZ-35 frequency meter, used for monitoring purposes, and to the input section of a multichannel pulse analyzer operating in the multiscalar regime, i. e., in a regime of sequential connection of the memory of the pulse analyzer to the input sections of the channels. The switching from one channel to another is effected by an external pulse from the control unit. The control unit ensures, together with an auxiliary F-5007 counter, the switching of the analyzer channels after the completion of a series of averaging over a given number of laser bursts. The level of averaging is fixed on the setting panel of the F-5007. The crystal under investigation is rotated simultaneously with the switching of the analyzer channels.

The information about the synchronism curves that is recorded in the analyzer memory can be partially or completely transferred to an automatic recorder, a digital press, or the digital indicator of the analyzer.

The above-described recording system is an improved version of the system used earlier in the experiments described in Refs. 11 and 13. The amplification factor for the current in the system is sufficient for the registration of the single-electron pulses of the photomultiplier. Owing to the gating of the analog-code converter, the probability of registering noise pulses is quite low.

§5. MEASUREMENT OF THE EFFECTIVE CUBIC SUSCEPTIBILITY AND THE DEGREE OF ANISOTROPY ANISOTROPY OF THE $\chi^{(3)}$ TENSOR IN A KDP CRYSTAL

In this section we present the results of the measurement of the quantity $\chi_{\text{eff}}^{(3)}$ and of the so-called anisotropy factor $\delta = \chi_{1111}^{(3)} - 3\chi_{1122}^{(3)}$ in a KDP crystal. The earlier published investigations^[8,14] do not enable us to determine these quantities with a sufficient degree of accuracy (see below).

Primarily, third-harmonic generation in a KDP crystal was investigated. Synchronous third-harmonic generation was observed in five directions, which correspond to the various types of interactions (see §2). The results are presented in Table I.^[1]

The quantity $\chi_{\text{eff}}^{(3)}$ was determined by us by means of comparative measurements of the intensity of the third harmonic excited in the direct and cascade processes.

We succeeded in expressing $\chi_{\text{eff}}^{(3)}$ (KDP) in units of d_{14}^2 (KDP), which enabled us to raise the measurement accuracy.

The KDP crystal does not possess an inversion center, and belongs to the $42m$ point group. The birefringence of this crystal allows us to obtain a synchronous third harmonic on the $\chi^{(3)}$ nonlinearity only on account of the $o_1o_1o_1e_3$ interaction (the synchronism angle $\theta_1 = 65^\circ$). The effective cubic susceptibility for this interaction is equal to

$$\chi_{\text{eff}}^{(3)}(\theta_1) = \frac{\cos \theta_1' \sin 4\varphi}{4} \left[\chi_{1111}^{(3)} - 3\chi_{1122}^{(3)} - \frac{16\pi d_{14}^2 \sin^2 \theta_1'}{n_2^* (3n_2^* - 2n_2^* - n_1^*)} \right], \quad (7)$$

where θ_1' is the angle between the Poynting vector and the z axis:

$$\text{tg } \theta_1' = (n^o/n^e)^2 \text{tg } \theta_1.$$

The intensity of the third-harmonic signal generated in the direction $\theta_1 = 65^\circ$ was equal to the intensity of the signal of this harmonic generated in the direction defined by the condition $k_2^e = 2k_1^o$. The effective third-order coupling constant for this process is expressible in terms of d_{14}^2 as follows:

$$\chi_{\text{eff}}^{(3)}(\theta_2) = \frac{8\pi^2 d_{14}^2 \sin^2 \theta_2'}{3n_2^* (n_2^* - n_1^o)} \sin^2 2\varphi. \quad (8)$$

The measurements were performed with KDP crystal plates of width 3 mm, cut, in the case of the $o_1o_1o_1e_3$ interaction, at angles $\theta_1 = 65^\circ$ and $\varphi = 22^\circ 30'$ and, in the $o_1o_1e_2$ interaction case, at angles $\theta_2 = 41^\circ$ and $\varphi = 45^\circ$.

Under our conditions (thin crystals, small pump divergence in comparison with the angular width of the synchronism), the expression (5) can be used. Substituting into (5) the expressions for the contractions $\langle \chi^{(2)} \rangle_j$ and the known values for the refractive indices, we obtain

$$\chi_{1111}^{(3)} - 3\chi_{1122}^{(3)} - 1930 d_{14}^2 = \pm 730 d_{14}^2 [I_3(\theta_1)/I_3(\theta_2)]^{1/4}.$$

The measurements showed that in the direction $\theta_1 = 65^\circ$ the third-harmonic intensity is lower than might have been expected if only the cascade process operated. Consequently, the direct and the cascade processes make contributions having unlike signs and partially compensating each other. For the intensity ratio $I_3(\theta_1)/I_3(\theta_2)$ we experimentally obtained the value $(8 \pm 2) \times 10^{-2}$. Then

$$\chi_{1111}^{(3)} - 3\chi_{1122}^{(3)} = + (1900 \pm 200) d_{14}^2.$$

Taking into account the fact that $d_{14}(\text{KDP}) = 1.04 \times 10^{-9}$ cgs esu,^[15] we obtain

$$\chi_{\text{eff}}^{(3)}(\theta_1) = (0.22 \pm 0.04) \cdot 10^{-16} \text{ cgs esu} \quad (9)$$

and

$$\chi_{1111}^{(3)} - 3\chi_{1122}^{(3)} = + (2.0 \pm 0.2) \cdot 10^{-15} \text{ cgs esu}.$$

Using the results of Ref. 4 and the experimental value, (9), obtained by us for the magnitude of the effective third-order nonlinear susceptibility in KDP, we can determine the degree of anisotropy of the $\chi^{(3)}$ tensor of the ADP crystal. The result is given in Table II.

TABLE II. Cubic nonlinear susceptibility values for crystals.

Crystal	$\alpha\beta\gamma\theta$	$\chi_{\alpha\beta\gamma\theta}^{(3)}$, 10^{-14} cgs esu		$\left(\frac{\chi_{1122}^{(3)}}{\chi_{1111}^{(3)}}\right)_{exp}$ ***	Literature
		Calculation*	Experiment		
NaBr	1111	+10.0	4.13±50%	-	[16]
NaF	1111	+0.12	+0.40±30%	-	[8, 17]
		-	0.33±50%	-	[16]
NaCl	1111	+4.0	1.3±20%	+0.43	[17, 18]
		-	+1.9±30%	-	[8, 17]
KCl	1111	+3.5	1.9±20%	+0.30	[18]
		-	+1.9±30%	-	[8, 17]
		-	1.3±50%	-	[16]
		-	-	+0.28	[19]
KBr	1111	+8.6	3.8±20%	+0.37	[18, 19]
		-	+4.5±30%	-	[8, 17]
		-	5.8±50%	-	[16]
LiF	1111	+0.22	0.34±15%	-	[20]
		-	0.20±20%	+0.45	[18, 19]
		-	+0.48±30%	-	[8, 17]
MgO	1111	+9.6	1.5±20%	+0.55	[18, 17]
		-	+3.8±30%	-	[8, 17]
CdS	1111	+164	160	-	[17]
ZnS	1111	+160	-	-	-
ZnO	1111	+9.0	-	-	-
CaCO ₃	3333	-	1.0±20%	-	[21]
	1111	+1.72	1.8±20%	-	[21]
	1133	-1.05	+0.44±25% **	-	-
	1122	+0.54	+0.20±25% **	-	-
	3222	-0.16	{ 0.05±30% ** 0.04	-	[15]
KDP	(1111)-3×(1122)	-	0.2±20% **	-	-
ADP	(1111)-3×(1122)	-	0.24±10% **	-	-

*The calculations were carried out on the basis of the Coulomb anharmonicity model.

**Present work. In computing the absolute values of $\chi^{(3)}$ we used the value $d_{14}(KDP) = 1.04 \times 10^9$ cgs esu.^[15]

***For the cubic crystals given here the Coulomb anharmonicity model gives $(\chi_{1122}^{(3)}/\chi_{1111}^{(3)})_{cal} = -0.5$.

§6. MEASUREMENT OF THE MAGNITUDES AND SIGNS OF THE COMPONENTS OF THE $\chi^{(3)}$ TENSOR OF THE CALCITE CRYSTAL

6.1. Measurement of the modulus of $\chi^{(3)}$

Calcite crystal plates of thickness 1.9 mm were cut out in such a way that the normal to the working face made for one plate an angle of $\theta = 37^\circ$, and for the other plate an angle of $\theta = 56^\circ$, with the crystal z axis. In all the measurements the radiation propagated in the crystal xz plane. The orientation of the rectangular system of coordinates with respect to the unit cell of calcite is shown in Fig. 4.

The birefringence of calcite allows all the three possible synchronous interactions to generate the third harmonic.^[22, 23] The coupling constants for the $o_1o_1o_1e_3$ ($\theta_1 = 29^\circ 11'$) and $o_1o_1e_2e_3$ ($\theta_2 = 35^\circ 45'$) interactions for the given radiation-propagation geometry in the crystal have respectively the following forms^[22]:

$$\chi_1(\theta_1) = \chi_{1122}^{(3)} \sin \theta_1', \quad (10)$$

$$\chi_2(\theta_2) = 3(\chi_{1122}^{(3)} \cos^2 \theta_2' + \chi_{1133}^{(3)} \sin^2 \theta_2'). \quad (11)$$

From a comparison of the third-harmonic intensities due to the $o_1o_1e_1e_3$ interaction in calcite and the interaction No. 7 (Table I) in a KDP crystal plate (of thickness 6 mm) we have

$$0.565 \chi_{1122}^{(3)} + 0.435 \chi_{1133}^{(3)} = (2840 \pm 300) d_{14}^2. \quad (12)$$

Comparing the third-harmonic intensities due to the $o_1o_1o_1e_3$ and $o_1o_1e_1e_3$ interactions in calcite, we obtain for the component $\chi_{3222}^{(3)}$ the expression

$$\chi_{3222}^{(3)} = (440 \pm 110) d_{14}^2.$$

To estimate directly the component $\chi_{1122}^{(3)}$ and $\chi_{1133}^{(3)}$, we must find the dependence of the expression (11) on the angle θ . For this purpose we investigated other four-photon interactions in calcite, interactions in which the fundamental laser radiation is used together with its second harmonic, produced in a LiNbO₃ crystal located in front of the calcite crystal.

In this case the four-photon processes in calcite lead to the generation of the third, fourth, and fifth harmonics, depending on the type of interaction:

$$2\omega + 2\omega - \omega = 3\omega, \quad 2\omega + \omega + \omega = 4\omega, \quad 2\omega + 2\omega + \omega = 5\omega.$$

From a comparison of the fourth-harmonic intensities for the $o_1e_1o_2e_4$ ($\theta_3 = 43^\circ 50'$) and $o_1o_1e_2e_4$ ($\theta_4 = 54^\circ 45'$) interactions we obtained

$$\chi_2(\theta_3)/\chi_2(\theta_4) = 0.90 \pm 0.03. \quad (13)$$

A comparison of the intensities of the third harmonic generated by the $o_2o_2e_1e_3$ ($\theta_5 = 17^\circ 31'$) and $o_2e_2o_1e_3$ ($\theta_6 = 32^\circ 45'$) interactions yields additional information about the variation of χ_2 with the angle θ :

$$\chi_2(\theta_5)/\chi_2(\theta_6) = 0.78 \pm 0.03. \quad (14)$$

Using the expressions (11)–(14), we found

$$\chi_{1122}^{(3)} = (1900 \pm 400) d_{14}^2, \quad \chi_{1133}^{(3)} = (4100 \pm 800) d_{14}^2.$$

These components have the same sign as in the expression (12).

6.2. Measurement of the sign of $\chi^{(3)}$

The signs of the measured components of $\chi^{(3)}$ were determined with the aid of the procedure described in §3. In front of the calcite crystal, set up for the $o_1o_1e_1e_3$ interaction, was placed a KDP crystal oriented at an angle corresponding to interaction No. 7 in Table I. When the crystal spacing was equal to 124 mm, the phase shift was $\Delta\alpha = 8\pi$, and we obtained experimentally a curve that corresponded to the case shown in Fig. 2c. Since for the crystal arrangement used $\rho = -1$ (see the formula (6)) and $\chi_{eff}^{(3)}(KDP) > 0$, for calcite ($0.565 \chi_{1122}^{(3)} + 0.435 \chi_{1133}^{(3)} > 0$) and, consequently (see (13) and (14)), the components $\chi_{1133}^{(3)}$ and $\chi_{1122}^{(3)}$ are positive.

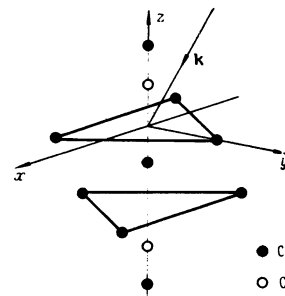


FIG. 4. Choice of rectangular system of coordinates with respect to the unit cell of calcite and the direction of propagation of the pumping wave in the crystal.

In measuring the sign of the component $\chi_{3222}^{(3)}$ for calcite, we encountered additional difficulties connected with the fact that, upon the rotation of the crystal through 180° about the y axis, or, which is the same thing, about the direction of the o -ray of the crystal, the shape of the synchronism interference curve changed, which corresponds to a "change" of the sign of $\chi_{3222}^{(3)}$. Therefore, particular attention was paid to the orientation of the coordinate system with respect to the direction of the pumping wave in the crystal (Fig. 4).

In determining the sign of $\chi_{3222}^{(3)}$ we used the interference of processes No. 5 and No. 14 in Table I with the $o_1o_1o_1e_3$ process in calcite. In the first case $\rho = -1$, in the second $\rho = +1$, and for both processes $\chi_{\text{eff}}^{(3)}(\text{KDP}) > 0$. Both interference measurements showed that $\chi_{3222}^{(3)} > 0$.

§7. THEORETICAL VALUES OF THE CUBIC NONLINEAR SUSCEPTIBILITIES

7.1. Theoretical models for the computation of $\chi^{(3)}$

As has already been indicated in the Introduction, the comprehensive exploitation of the cubic nonlinear susceptibilities is only beginning; therefore, we can compare our experimental results with two models. The first of them is the Boling-Glass-Owyong (BGO) semi-phenomenological rule^[9] and the second, developed to a considerable extent in the present paper, is the Coulomb anharmonicity model.^[10]

The scheme of computation on the basis of the BGO rules is described in Ref. 9, where the values of $\chi_{1111}^{(3)}$ in a number of types of glass are computed. This model was first used to compute $\chi^{(3)}$ for CaCO_3 and CaF_2 crystals and diamond by Levenson and Bloembergen.^[21] We have computed $\chi_{1111}^{(3)}$ on the basis of this model for all the crystals for which experimental data exist. The experimental data and the theoretical results obtained on the basis of the BGO rule are compared in Fig. 5.

7.2. The Coulomb anharmonicity model

The Coulomb anharmonicity model was proposed by Meisner^[10] for the computation of the quadratic susceptibility of crystals. In this model the entire nonlinearity is related to the anharmonic motion of the shell charge relative to its core. A distinctive feature of the model is the correct allowance made for the local electric fields acting on the ions in the lattice.

Let us, for simplicity, consider the one-dimensional case, i. e., the case when all the ions are located on the x axis and the external field E is also directed along this axis. The equation of motion of the i -th shell under the action of the fields of the charges surrounding it has the following form:

$$m_i \ddot{x}_i + \sum_{k=1}^m R_{ik}(x_k - x_i) = a_i \mathcal{E}_i(t, x_1 - x_i, x_2 - x_i, \dots), \quad (15)$$

where the x_i are the coordinates of the ion shells, m_i and a_i are the mass and charge of the shell of the i -th ion, and \mathcal{E}_i is the local field at the point i . The sum on

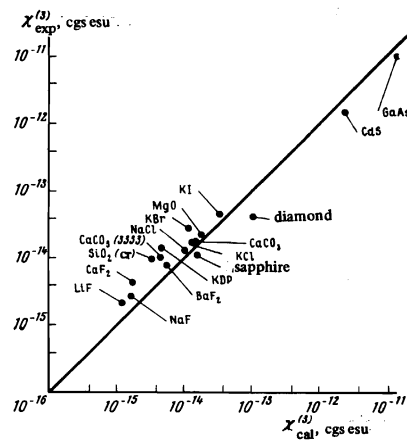


FIG. 5. Comparison of the experimental $\chi^{(3)}$ values for crystals with the values computed on the basis of the BGO rule.^[9] The experimental $\chi^{(3)}$ -component values are plotted along the ordinate axis; the calculated values, along the abscissa axis.

the left-hand side of Eq. (15) represents the short-range force. In the Coulomb anharmonicity model R_{ik} is assumed to be a constant, not depending on the shell spacing.

Thus, the solution of the problem (15) is connected with the computation of the intracrystalline field.^[24] The local field acting on the i -th shell consists of three parts: the external field (E), the field (\mathcal{E}') of the shells located in the Lorentz cavity, and the field (\mathcal{E}'') due to the charges outside the Lorentz cavity:

$$\mathcal{E}'' = \beta \sum_{k=1}^m N_k \mu_k;$$

here β is the Lorentz factor, N_k is the number of shells of the k -th type in a unit volume, and μ_k is the dipole moment of the shell of the k -th ion.

Let us find the field \mathcal{E}' by summing the fields of all the ions in the Lorentz cavity. The Coulomb potential of the shells of the ions of the k -th type relative to the i -th ion will be equal to

$$\varphi_i = \sum_{\pi} \sum_{j=1}^{N_k} \frac{a_k}{|x_j - x_i|} \quad (16)$$

(\sum_{π} denotes summation over the unit cells within the boundaries of the Lorentz cavity). The potential φ_i (and, consequently, the field \mathcal{E}') at the point i depends on the small displacements of the shell charges. Therefore, it is more convenient to expand the field at the point i in powers of the displacements of the shells surrounding it:

$$\mathcal{E}_{ik}' = a_k (f_{ik}^{(0)} + f_{ik}^{(1)} w_k + \dots + f_{ik}^{(N)} w_k^N + \dots). \quad (17)$$

In (17) w_k is the displacement of the shell of the k -th ion; $w_k = x_k - x_k^{(0)}$, $x_k^{(0)}$ being the coordinate of the k -th ion shell in the absence of an external field, and the

$$f_{ik}^{(N)} = \frac{1}{N!} \sum_{\pi} \sum_{j=1}^{N_k} \frac{\partial^{N+1}}{\partial x_j^{N+1}} \left| \frac{1}{x_j - x_i^{(0)}} \right|_{x_j = x_j^{(0)}} \quad (18)$$

are unidimensional structure coefficients of the local field.^[24]

The coefficients $f_{ik}^{(N)}$ depend only on the ion coordinates, and at the present level of computer technology their computation presents no problem. In the case of odd N the matrix $f_{ik}^{(N)}$ is symmetric, and in the case of even N antisymmetric. To find the total field, however, we sum over all the types of ions in the crystal. Then

$$\mathcal{E}_i = E(t) + \sum_{k=1}^m [f_{ik}^{(N)} + g_{ik} w_k + f_{ik}^{(2)} w_k^2 + \dots + f_{ik}^{(N)} w_k^N + \dots] a_k, \quad (19)$$

where $g_{ik} = N_k \beta + f_{ik}^{(1)}$.

We assume the external field $E(t)$ to be harmonic: $E(t) = E(\omega) e^{i\omega t}$. The system of equations (15) is solved by the method of perturbations:

$$w_i(t) = w_i^{(1)}(t) + w_i^{(2)}(t), \quad w_i^{(1)}(t) = w_i^{(1)}(\omega) e^{i\omega t}, \\ w_i^{(2)}(t) = \sum_{n=1}^{\infty} w_i^{(2)}(N\omega) e^{iN\omega t}.$$

In the linear approximation, the solution, $w_i^{(1)}(\omega)$, to (15) can be expressed in terms of the linear polarizability α_i , using the connection between the shell model and the polarizable-ion model^[25]

$$w_i^{(1)}(\omega) = \frac{\alpha_i \mathcal{E}_i}{a_i} = \frac{\alpha_i A_i}{a_i} E(\omega); \quad (20)$$

the constants A_i are obtained here from the solution of the system of equations for the local field^[24]

$$\mathcal{E}_i = E(\omega) + \sum_{k=1}^m g_{ik} \alpha_k \mathcal{E}_k.$$

Retaining in the expression, (19), for the local field the term containing $(w_k^{(1)})^N$, and using (20), we obtain the solution for $w_i^{(1)}(N\omega)$:

$$w_i^{(1)}(N\omega) = \alpha_i(N\omega) \frac{A_i}{a_i} E^N(\omega) \sum_{k=1}^m f_{ik}^{(N)} \frac{\alpha_k^N A_k^N}{a_k^{N-1}}. \quad (21)$$

Let us define the nonlinear susceptibility $\chi^{(N)}$ in the usual manner:

$$P_a^{(N)}(N\omega) = \chi_{\alpha\beta\gamma\dots\theta}^{(N)} E_\alpha(\omega) E_\beta(\omega) \dots E_\theta(\omega) \\ = \sum_i N_i w_i^{(1)}(N\omega) a_i.$$

Then

$$\chi_{\alpha\alpha\dots\alpha}^{(N)} = \sum_{i=1}^m N_i \alpha_i(N\omega) A_i \sum_{k=1}^m f_{ik}^{(N)} [\alpha_k(\omega) A_k]^N a_i^{1-N}. \quad (22)$$

Meisner^[10] has carried out the computation of $\chi^{(2)}$ from (22) for a number of crystals. For the computation of the odd-order nonlinear susceptibilities we can simplify the formula (22). The point is that there do not exist at present reliable methods of obtaining accurate values for the polarizabilities α_k and the charges a_k . Therefore, it is more convenient to replace $\alpha_k A_k$ by the effective susceptibility $\kappa = \chi^{(1)}/N_0$ (N_0 is the number of ions in a unit volume) and a_k by an effective charge a ; we assume κ and a are the same for all the ions in the

lattice, i. e., we shall, in the linear approximation, assume that all the electronic oscillators are equivalent. Then, in computing the odd-order susceptibilities, we can use in place of (22) the formula

$$\chi_{\alpha\alpha\dots\alpha}^{(N)} = \frac{\chi_{\alpha\alpha}^{(1)}(N\omega) [\chi_{\alpha\alpha}^{(1)}(\omega)]^N}{N_0^{N+1} a^{N-1}} \sum_{i,k=1}^m N_i f_{ik}^{(N)}. \quad (23)$$

Let us define the effective charge, a , of a shell as one half the charge of the bond formed by the ions A and B , the charge of the bond being, according to Levine,^[26] equal to

$$a_b = n_s e (1/\epsilon + 1/s f_c),$$

where n_s is the number of electrons per bond in the s and p states divided by the number of bonds in one formula unit, ϵ is the low-frequency value of the square of the refractive index, and f_c is the degree of covalence of the bond. For the majority of the crystals considered in the present work the f_c values are known.

Thus, we determined all the free parameters, and could use Eq. (23) to compute the components of the $\chi^{(2N-1)}$ tensors. Let us emphasize once again that the considered approach cannot be used to compute $\chi^{(2N)}$, since, on account of the antisymmetric nature of the matrix $f_{ik}^{(2N)}$, we obtain for the case when the A_i and α_i are the same for all the ions in the lattice $\chi^{(2N)} \equiv 0$. To compute the even-rank susceptibilities, we must use the formula (22).

The formula (23) can easily be generalized to the case of an arbitrary tensor component and a nondegenerate nonlinear interaction of the light waves:

$$\chi_{\alpha\beta\gamma\dots\theta}^{(2N-1)}(\omega; \omega_1, \omega_2, \dots, \omega_{2N-1}) \\ = \frac{1}{N_0^{2N} a^{2N-2}} \sum_{i,k=1}^m N_i f_{i\alpha\beta\gamma\dots\theta}^{(2N-1)} \chi_{\alpha\alpha}^{(1)}(\omega) \chi_{\beta\beta}^{(1)}(\omega_1) \chi_{\gamma\gamma}^{(1)}(\omega_2) \dots \chi_{\theta\theta}^{(1)}(\omega_{2N-1}); \\ \omega = \sum_{i=1}^{2N-1} \omega_i. \quad (24)$$

The formula (24) has the structure of the Miller rule.^[27] However, in our case the Miller "constant" $\Delta_{\alpha\beta\gamma\dots\theta}^{(2N-1)}$ depends on the crystal structure, the number of ions in a unit volume, and the effective charge. The expression (24) allows us to compute, besides the magnitude, the sign of $\chi^{(2N-1)}$.

7.3. Computation of the $\chi^{(3)}$ of crystals on the basis of the Coulomb anharmonicity model

a) *Crystals of the NaCl type.* Crystals with the NaCl structure are cubic crystals with an inversion center, and have two independent $\chi^{(3)}$ -tensor components: $\chi_{1111}^{(3)}$ and $\chi_{1122}^{(3)}$. In computing these components, we calculated the elements of the matrices $f_{ik,1111}^{(3)}$ and $f_{ik,1122}^{(3)}$ on a computer for the actual locations of the ions in the lattice. The degree, f_c , of covalence of the bond was taken in accordance with the data collected in Born and Huang's book.^[24] The results of the computation of $\chi_{1111}^{(3)}$ from (23) and the experimental data are presented in Table II and Fig. 6. It is not difficult to see that the Coulomb

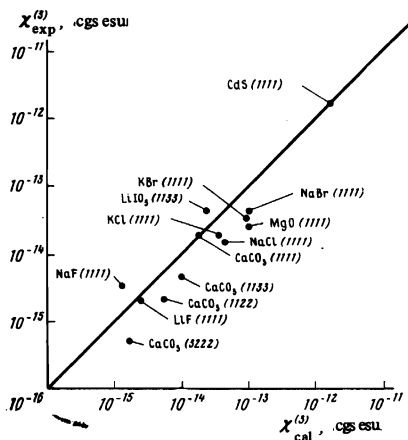


FIG. 6. Comparison of the experimental $\chi_{\alpha\beta\gamma\theta}^{(3)}$ values for crystals with values computed on the basis of the Coulomb-anharmonicity model. The indices of the components are indicated in the brackets.

anharmonicity model leads to satisfactory quantitative agreement with experiment for the $\chi_{1111}^{(2)}$ component, and correctly gives its sign. The quantitative disagreement with experiment is connected with the inaccuracy in the determination of the quantities κ and a . However, there are other more serious causes.

The theory for cubic crystals should lead to the inequality of $\chi_{1111}^{(3)}$ and $3\chi_{1122}^{(3)}$ ($\delta \neq 0$). The difference between these two quantities is an important characteristic of cubic crystals, providing direct information about the anisotropy of the electron shells of cubic crystals. This information cannot be obtained from the measurement of the linear properties of the medium. The Coulomb anharmonicity model, owing to the fact that it correctly allows for the anisotropy of the long-range (Coulomb) forces, i. e., for the anisotropy of the local field ($f_{iR,1111}^{(3)} \neq 3f_{iR,1122}^{(3)}$), leads to the result that $\chi_{1111}^{(3)}$ is different from $3\chi_{1122}^{(3)}$. Indeed, for all diatomic cubic crystals, $f_{iR,1111}^{(3)} = -2f_{iR,1122}^{(3)}$; consequently,

$$\chi_{1122}^{(3)}/\chi_{1111}^{(3)} = -0.5.$$

The obtained values for this ratio are in satisfactory quantitative agreement with experiment (see Table II), but do not coincide in sign (experiment yields the plus sign). The discrepancy is, apparently, due to the fact that we neglected the anharmonicity of the short-range forces in the computation of $\chi^{(3)}$. In particular, the need to take the non-Coulomb forces into account is indicated also by the bound-charge model,^[7] within the framework of which the components of the $\chi^{(3)}$ tensor for Si, GaAs, and Ge crystals were calculated. However, allowance for the short-range forces involves considerable difficulties, and the consideration of this problem falls outside the limits of the present work.

b) *Wurtzite crystals.* Crystals with the wurtzite structure belong to the hexagonal system, and do not have a center of inversion. We shall restrict ourselves to the computation of the $\chi_{1111}^{(3)}$ component for CdS, ZnS, and ZnO crystals. The experimental value is known only for the CdS crystal. This experimental value and the

theoretical $\chi_{1111}^{(3)}$ values for CdS, ZnS, and ZnO crystals are given in Table II. Notice that there is excellent agreement between theory and experiment for the CdS crystal.

c) *Calcite.* The CaCO_3 crystal structure is considerably more complex than the structure of the above-considered crystals. It is sufficient to note just the fact that the unit cell contains thirty atoms. However, the computation of the $\chi_{\alpha\beta\gamma\theta}^{(3)}$ components for calcite does not differ in any way from the computation of the $\chi^{(3)}$ tensor of crystals with the NaCl or CdS structure. This is one of the advantages of the above-developed method.

In computing the $\chi_{\alpha\beta\gamma\theta}^{(3)}$ components for CaCO_3 , we calculated the elements of the matrices $f_{iR,\alpha\beta\gamma\theta}^{(3)}$ for the actual positions of the ions in the lattice. Further, we must have for the computation data on the degree of ionicity of CaCO_3 . These data are lacking; therefore, we used the experimental value for $\chi_{3333}^{(3)}$ [21] to estimate a . Let us note that, as calculations have shown, the sign of the $\chi_{3333}^{(3)}$ component does not change when the parameter a is varied within broad limits.

The computed values of the components and the experimental data are presented in Table II and Fig. 6. Let us note first of all that, in accordance with the symmetry of the CaCO_3 lattice, the following equalities should be fulfilled:

$$\chi_{1122}^{(3)} = 1/2\chi_{1111}^{(3)}, \quad \chi_{3311}^{(3)} = -\chi_{3322}^{(3)}.$$

Equation (24) leads to results that agree with these calcite-crystal symmetry requirements. Further, according to the experimental data, the difference between the magnitudes of the $\chi_{1111}^{(3)}$ and $\chi_{3222}^{(3)}$ components in CaCO_3 exceeds an order of magnitude, and this is in agreement with the theoretical estimates. From the theoretical standpoint this is due to the difference in magnitude of $f_{iR,1111}^{(3)}$ and $f_{iR,3222}^{(3)}$. In other words, the anharmonicity of the shell motion is greater in the (010) plane than in the (011) plane.

All the computed $\chi_{\alpha\beta\gamma\theta}^{(3)}$ components for calcite are in satisfactory quantitative agreement with experiment.

d) *KDP and ADP crystals.* For these crystals we compute from (24) only the following type of ratio

$$\chi^* = (\chi_{1111}^{(3)} - 3\chi_{1122}^{(3)})_{\text{ADP}} / (\chi_{1111}^{(3)} - 3\chi_{1122}^{(3)})_{\text{KDP}}.$$

This is due not to some kind of fundamental difficulties encountered in the computation of the $\chi^{(3)}$ components for crystals with the KDP structure, but to the fact that χ^* can be considered to be charge independent ($a_{\text{KDP}} \sim a_{\text{ADP}}$). The result obtained for χ^* agrees excellently with experiment:

$$\chi_{\text{exp}}^* = 1.20, \quad \chi_{\text{cal}}^* = 1.24.$$

§8. CONCLUSION

8.1. Comparison of the calculated and experimental data on $\chi^{(3)}$

In our opinion the main criteria that we need to be guided by in comparing the calculated and experimental

data are the following comparative characteristics: a) quantitative agreement, b) the correct representation of the relation between the χ components for the same crystal, c) the sign of the components.

a) *Quantitative agreement.* The experimental data and the theoretical data obtained on the basis of the Coulomb anharmonicity model are compared in Fig. 6. The agreement with experiment is good. However, this should not be considered the principal merit of the theory. So simple a model as the GBO rule^[9] gives, when the quantities in question are the diagonal elements of $\chi^{(3)}$, even somewhat better agreement with experiment than the Coulomb anharmonicity model (see Fig. 5).

b) *Relation between the components.* Depending on the crystal symmetry, the $\chi^{(3)}$ tensor has several independent components. The difference between one component and another is connected with the anisotropy in the properties of the crystal, and such type of measurement yields important information about the types of bonds in the crystal, about the ellipticity of the electron orbits, etc. Therefore, the opportunity for the present model to correctly describe the relation between the components is quite a fundamental aspect of the model.

For cubic crystals the component $\chi_{1111}^{(3)} \neq 3\chi_{1122}^{(3)}$. On the basis of the BGO rule it is impossible to find the relation between these two components. The bound-charge model^[7] correctly describes this relation for GaAs, Ge, and Si: $\chi_{1122}^{(3)}/\chi_{1111}^{(3)} = 0.75$ (the experimental value is 0.5). According to the Coulomb anharmonicity model, $|\chi_{1122}^{(3)}/\chi_{1111}^{(3)}| = 0.5$, which is close to the experimental values (see Table II).

c) *The sign of the components.* The sign of the susceptibilities also carries a considerable amount of information about the bonds between ions in crystals.^[28] The BGO rule allows us to obtain only the modulus of the quantity $\chi^{(3)}$. The bound-charge and Coulomb anharmonicity models allow us to compute the sign of $\chi^{(3)}$. As can be seen from Table II, the Coulomb-anharmonicity model gives the correct sign in the case of the diagonal elements of $\chi^{(3)}$. For components of the type $\chi_{1122}^{(3)}$ and $\chi_{1133}^{(3)}$ the computed sign is the opposite of the experimentally measured sign. This fact indicates the need for further improvement of the model and, in particular, for allowance for the non-Coulomb corrections.

8.2. Comparison of the experimental data on $\chi^{(3)}$ with the data obtained in other investigations

The cubic susceptibility of the calcite crystal has been investigated in a number of experiments.^[14,21,18,29,30] In the experiments described in Refs. 14 and 18, the measurements of the components were carried out on the basis of absolute measurements of the intensity of the third harmonic (TH) generated in the synchronous regime.

In the experiment described in Ref. 29 the estimate $\chi_{3222}^{(3)} = 2.2 \times 10^{-14}$ cgs esu was obtained on the basis of second-harmonic intensity measurements in the presence of a constant electric field. In the investigations published in Refs. 21 and 30 the measurements of the

$\chi^{(3)}$ components for calcite were carried out, using the method of Raman-active scattering spectroscopy (the results are given in the table). The experimental results of these investigations poorly agree with each other. The difficulties that we encountered in the estimation of $\chi^{(5)}$ in the calcite crystal^[11] were connected with this circumstance. Our result for the $\chi_{3222}^{(3)}$ component agrees very well with the result obtained for this component in Ref. 18. The result for $\chi_{1122}^{(3)}$ is three times smaller than the value obtained for $\frac{1}{3}\chi_{1111}^{(3)}$ in Ref. 21 by the method of Raman-active scattering spectroscopy. In the investigation published in Ref. 30 it was found by the method of Raman-active scattering spectroscopy that the $\chi^{(3)}$ components for calcite satisfy the relation

$$0.22\chi_{1133}^{(3)} + 0.78\chi_{1122}^{(3)} > 0.$$

In the present work we have obtained by the method of synchronous third-harmonic generation that

$$0.44\chi_{1133}^{(3)} + 0.66\chi_{1122}^{(3)} > 0.$$

The effective cubic susceptibility of the KDP crystal for the $o_1o_1o_1e_3$ interaction has been measured earlier.^[6,14] In Ref. 14 it was found by the method of absolute measurements of the TH intensity that $\chi_{\text{eff}}^{(3)}(\text{KDP}) = 10^{-16}$ cgs esu. Using the value for the ratio $\chi_{\text{eff}}^{(3)}(\text{KDP})/\chi_{\text{eff}}^{(3)}(\text{ADP})$ obtained in Ref. 6 and the measured—in the same manner as in Ref. 14—value for $\chi_{\text{eff}}^{(3)}(\text{ADP})$ from Ref. 31, we find that

$$\chi_{\text{eff}}^{(3)}(\text{KDP}) = 5 \cdot 10^{-16} \text{ cgs esu}.$$

We think that the value given in the present paper for $\chi_{\text{eff}}^{(3)}(\text{KDP})$ is closer to the true value since it has been obtained by a method that guarantees a higher accuracy.

The value of the anisotropy factor, δ , has, however, been obtained for the first time in our work.

8.3. Estimates for the $\chi_{322222}^{(3)}$ component of the fifth-order nonlinear susceptibility tensor of the calcite crystal

The results obtained in the cubic-susceptibility measurements performed in the present work can also be used to interpret the recent experiments in which nonlinear effects of fourth and fifth order in the field were studied. Specifically, of indubitable interest is the estimation of the fifth-order nonlinear-susceptibility components from the experiments on fifth-harmonic generation in calcite^[11]; as in the case of third-harmonic generation in noncentrosymmetric media, the contribution to the effective fifth-order nonlinearity is made by lower-order nonlinearities: in the present case by $\chi^{(3)}$. Earlier (see Ref. 11) we encountered difficulties in the estimation of the $\chi_{322222}^{(5)}$ component because of the lack of firmly established data for $\chi_{1111}^{(3)}$ and $\chi_{3222}^{(3)}$. It seems to us that the most correct thing to do in estimating $\chi_{322222}^{(5)}$ is to use the experimental values for $\chi^{(3)}$ obtained in the present work, to wit,

$$\chi_{1111}^{(3)} = 6 \cdot 10^{-15} \text{ cgs esu}, \quad \chi_{3222}^{(3)} = 5 \cdot 10^{-16} \text{ cgs esu}.$$

Then for the value of the $\chi_{322222}^{(5)}$ component we obtain

$$|\chi_{32222}^{(5)}(\text{exp})| = \begin{cases} 2.6 \cdot 10^{-28} \text{ cgs esu}, & \chi_{3222}^{(3)} \chi_{32222}^{(5)} < 0 \\ 14 \cdot 10^{-28} \text{ cgs esu}, & \chi_{3222}^{(3)} \chi_{32222}^{(5)} > 0 \end{cases}$$

The nonlinear-susceptibility theory developed in §6 can be used to compute the fifth-order nonlinear susceptibilities. The calculation of the $\chi_{32222}^{(5)}$ component from the formula (24) yields

$$\chi_{32222}^{(5)}(\text{cal}) = +0.36 \cdot 10^{-28} \text{ cgs esu.}$$

According to the Coulomb anharmonicity model, the product $\chi_{3222}^{(3)} \chi_{32222}^{(5)} < 0$. Thus, we should choose from the two experimental values the smaller value, which, moreover, is closer to the theoretical $\chi_{32222}^{(5)}$ value.

¹⁾In the table we use the standard notation for the types of interaction. The symbols *o* and *e* represent the ordinary and extraordinary wave in the crystal.

¹⁾J. F. Ward and C. H. G. New, *Phys. Rev.* **185**, 57 (1969).

²⁾B. F. Levine and C. G. Bethea, *J. Chem. Phys.* **63**, 2666 (1975).

³⁾E. Yablonoitch, C. Flytzanis, and N. Bloembergen, *Phys. Rev. Lett.* **29**, 865 (1972).

⁴⁾S. D. Kramer, F. Parsons, and N. Bloembergen, *Phys. Rev.* **B9**, 1853 (1974).

⁵⁾J. Wynne, *Phys. Rev.* **178**, 1295 (1969).

⁶⁾M. Okada, *Appl. Phys. Lett.* **18**, 451 (1971).

⁷⁾D. S. Chemla, R. F. Begley, and R. I. Byer, *IEEE J. Quantum Electron.* **QE-10**, 71 (1974).

⁸⁾C. C. Wang and E. L. Baardsen, *Phys. Rev.* **185**, 1079 (1969).

⁹⁾N. L. Boling, A. J. Glass, and A. Owyong, "An Empirical Relationship for Predicting Nonlinear Refractive Index Changes in Optical Solids," preprint, University of California, USA, 1974.

¹⁰⁾L. B. Meisner, *Zh. Eksp. Teor. Fiz.* **69**, 2101 (1975) [*Sov. Phys. JETP* **42**, 1068 (1976)].

¹¹⁾S. A. Akhmanov, A. N. Dubovik, S. M. Saltiel, I. V. Tomov,

and V. G. Tunkin, *Pis'ma Zh. Eksp. Teor. Fiz.* **20**, 264 (1974) [*JETP Lett.* **20**, 117 (1974)].

¹²⁾S. A. Akhmanov and R. V. Khokhlov, *Problemy nelineinoi optiki* (Problems of Nonlinear Optics), VINITI, 1964 (Eng. Transl., Gordon & Breach, New York, 1972).

¹³⁾S. A. Akhmanov, V. A. Martynov, S. M. Saltiel, and V. G. Tunkin, *Pis'ma Zh. Eksp. Teor. Fiz.* **22**, 143 (1975) [*JETP Lett.* **22**, 65 (1975)].

¹⁴⁾I. V. Tomov, *Dissertatsiya* (Dissertation), MGU, 1970.

¹⁵⁾B. F. Levine and C. G. Bethea, *Appl. Phys. Lett.* **20**, 272 (1972).

¹⁶⁾W. L. Smith, J. H. Rechtel, and N. Bloembergen, *Phys. Rev.* **B12**, 706 (1975).

¹⁷⁾C. C. Wang, *Phys. Rev.* **B2**, 2045 (1970).

¹⁸⁾P. D. Maker and R. W. Terhune, *Phys. Rev.* **137**, A801 (1965).

¹⁹⁾W. K. Burns and N. Bloembergen, *Phys. Rev.* **B4**, 3437 (1971).

²⁰⁾M. D. Levenson, *IEEE J. Quantum Electron.* **QE-10**, 110 (1974).

²¹⁾M. Levenson and N. Bloembergen, *Phys. Rev.* **B10**, 4447 (1974).

²²⁾J. E. Midwinter and J. Warner, *Br. J. Appl. Phys.* **16**, 1667 (1965).

²³⁾I. V. Tomov and A. N. Sukhorukov, *Zh. Eksp. Teor. Fiz.* **58**, 1626 (1970) [*Sov. Phys. JETP* **31**, 872 (1970)].

²⁴⁾M. Born and K. Huang, *Dynamical Theory of Crystal Lattices*, Oxford University Press, Oxford, 1954 (Russ. Transl., IIL, 1958).

²⁵⁾R. L. Kelly, *Phys. Rev.* **151**, 721 (1966).

²⁶⁾B. F. Levine, *Phys. Rev.* **B7**, 2600 (1973).

²⁷⁾R. C. Miller, *Appl. Phys. Lett.* **5**, 17 (1964).

²⁸⁾C. L. Tang, *IEEE J. Quantum Electron.* **QE-9**, 755 (1973).

²⁹⁾J. E. Bjorkholm and A. E. Siegman, *Phys. Rev.* **154**, 851 (1967).

³⁰⁾S. A. Akhmanov and N. I. Koroteev, *Zh. Eksp. Teor. Fiz.* **67**, 1306 (1974) [*Sov. Phys. JETP* **40**, 650 (1975)].

³¹⁾C. C. Wang and E. L. Baardsen, *Appl. Phys. Lett.* **15**, 396 (1969).

Translated by A. K. Ageyi